ied previously[9] and the results have been applied to the evaluation of the dihedral angle between the two anthracene rings in the ground and electronically excited states.[20] The values obtained are 85–100° at the ground state and 75 ± 5° or 113 ± 5° at the excited state (two different values can be assigned to the dihedral angle in the excited state to fit the experimental data). Also in this case the anisotropy factors of absorption and emission assume equal magnitude at the overlap region of absorption and emission when studied in a very highly viscous mixture of poly(methyl methacrylate) in chloroform (see Figure 9), which indicates a freezing of the ground state conformation by the viscous solvent.

Conclusion

The optical rotatory power of all the seven cyclic dipeptides studied is different when in the ground state and in the electronically excited state, indicating a difference in molecular conformation in the two states. The change in conformation reflected by the optical activity is very fast compared to the fluorescence decay rate even in glycerol but is arrested in extremely highly viscous solvents. Overall rotational Brownian motion of the excited chromophores, as reflected by the linear polarization of the fluorescence, is shown to be a different and slower process, since it is appreciably hindered in glycerol. The relaxation processes observed by Donzel, et al.,[8] in the nanosecond time range in fluid media seem to be still slower processes of a still different nature, since they were observed under conditions where rotational relaxation is complete within the fluorescence

lifetime. We could not detect any linear polarization in dioxane solution.

References and Notes

(1) J. Caillet, B. Pullman, and B. Malgret, *Biopolymers*, **10**, 221 (1971).
(2) R. Chandrasekaran, A. V. Lakshminarayanan, P. Mohanakrishnan, and G. N. Ramachandran, *Biopolymers*, **12**, 1421 (1973).
(3) L. E. Webb and C.-F. Lin, *J. Amer. Chem. Soc.*, **93**, 3818 (1971).
(4) K. D. Kopple and D. H. Marr, *J. Amer. Chem. Soc.*, **89**, 6193 (1967).
(5) K. D. Kopple and M. Ohniski, *J. Amer. Chem. Soc.*, **91**, 962 (1969).
(6) H. Edelhoch, R. E. Lippoldt, and M. Wilchek, *J. Biol. Chem.*, **243**, 4799 (1968).
(7) E. H. Strickland, M. Wilchek, J. Horwitz, and C. Billups, *J. Biol. Chem.*, **245**, 4168 (1970).
(8) B. Donzel, P. Gauduchon, and Ph. Wahl, *J. Amer. Chem. Soc.*, **96**, 801 (1974).
(9) A. Gafni and I. Z. Steinberg, *Photochem. Photobiol.*, **15**, 93 (1972).
(10) J. Schlessinger and I. Z. Steinberg, *Proc. Nat. Acad. Sci. U. S.*, **67**, 769 (1972).
(11) C. A. Emeis and L. J. Oosteroff, *J. Chem. Phys.*, **54**, 4809 (1971).
(12) A. Gafni, J. Schlessinger, and I. Z. Steinberg, *Isr. J. Chem.*, **11**, 423 (1973).
(13) A. Gafni and I. Z. Steinberg, *Biochemistry*, **13**, 800 (1974).
(14) S. Veinberg, S. Shaltiel, and I. Z. Steinberg, *Isr. J. Chem.*, **12**, 421 (1974).
(15) C. K. Luk and F. S. Richardson, *J. Amer. Chem. Soc.*, **96**, 2006 (1974).
(16) I. Z. Steinberg in "Concepts in Biochemical Fluorescence," R. Chen and H. Edelhoch, Ed., Marcel Dekker, New York, N.Y., 1974.
(17) G. Weber and B. Bablouzian, *J. Biol. Chem.*, **241**, 2558 (1966).
(18) I. Z. Steinberg and A. Gafni, *Rev. Sci. Instrum.*, **43**, 409 (1972).
(19) A. Moscowitz in "Modern Quantum Chemistry," O. Sinanoglu, Ed., Part III, Academic Press, New York, N.Y., 1965, pp 31–44.
(20) J. Schlessinger and A. Warshel, *Chem. Phys. Lett.*, in press.

Spectra and Structure of Organogermanes. XVII.[1] Microwave Spectrum, Structure, Dipole Moment, and Internal Rotational Barrier of Vinylgermane

J. R. Durig,*[2] K. L. Kizer,[3] and Y. S. Li

Contribution from the Department of Chemistry, University of South Carolina, Columbia, South Carolina 29208. Received May 22, 1974

Abstract: The microwave spectra of ten isotopic species of vinylgermane have been recorded in the region between 12.4 and 40.0 GHz. From a least-squares fit of the 25 rotational constants and an assumed structure for the vinyl group, except for the C=C bond distance, the following structural parameters were calculated: $r(C=C) = 1.347$Å, $r(Ge—H) = 1.521$Å, $r(Ge—C) = 1.926$Å, $\angle(CCGe) = 122°54'$, $\angle(CGeH) = 110°42'$. The barrier to internal rotation of the germyl group has been determined to be 1238 ± 57 cal/mol from the ground and excited state splittings of the rotational transitions. Quadratic Stark effect measurements on the $J = 3 \leftarrow 2$ transitions gave $|\mu_a| = 0.49 \pm 0.02$, $|\mu_b| = 0.12 \pm 0.02$, and $|\mu_{total}| = 0.50 \pm 0.03$ D. An upper limit of 2.8 MHz has been set on the quadrupole coupling constant, $|\chi_{aa}|$, for ^{73}Ge isotope from a measurement of the line width of the transitions due to this isotopic species.

There have been few structural studies of organogermanium compounds in the gaseous state[4-12] although there have been some rather large variations reported[13] for the Ge–C distances for some of these compounds. As a continuation of our earlier studies of a series of organogermanes, we have investigated the microwave spectrum of vinylgermane. From vibrational studies[14] on CH_2CHGeH_3 and CH_2CHGeD_3, it was concluded that the molecule has C_s symmetry. However, no torsional frequency for the germyl group was observed for either molecule.

The microwave spectra of propylene[15-17] and vinylsilane[18] have been investigated and their structures and bar-

riers to internal rotation were determined. The relatively large difference in barriers between ethane[19] (2.93 kcal/mol) and propylene[17] (1.98 kcal/mol) vs. the small difference in barriers between methylsilane[20] (1.67 kcal/mol) and vinylsilane[18] (1.50 kcal/mol) has been attributed to hyperconjugation. A comparison of the dipole moment and the corresponding C–C single bond distances in ethane and propylene also tends to favor hyperconjugation in propylene. Since the microwave spectrum of methylgermane[4-6] was investigated and its structure, barriers to internal rotation, and electric dipole moment were determined, it was felt that the study of the microwave spectrum of vinylgermane might

Table I. Observed Ground-State Transition Frequencies (MHz) for Vinylgermane[a]

| Transition | —CH$_2$CH^{70}GeH$_3$— | | —CH$_2$CH^{72}GeH$_3$— | | —CH$_2$CH^{73}GeH$_3$— | | —CH$_2$CH^{74}GeH$_3$— | | —CH$_3$CH^{76}GeH$_2$— | |
	ν (obsd)	Δν[b]	ν (obsd)	Δν[b]	ν (obsd)	Δν[b]	ν (obsd)	Δν[b]	ν (obsd)	Δν[b]
$2_{12} \leftarrow 1_{11}$[c]	14,767.64	0.03	14,681.92	0.02	14,640.60	0.05	14,600.34	0.01	14,522.66	0.03
$2_{02} \leftarrow 1_{01}$[c]	15,024.40	−0.06	14,935.73	−0.04	14,892.91	−0.10	14,851.45	−0.01	14,771.00	−0.06
$2_{11} \leftarrow 1_{10}$[c]	15,284.80	0.03	15,193.04	0.02	15,148.85	0.05	15,105.89	0.00	15,022.76	0.03
$3_{13} \leftarrow 2_{12}$	22,150.33	−0.01	22,021.72	−0.08	21,959.66	−0.12	21,899.39	−0.08	21,782.89	−0.05
$3_{03} \leftarrow 2_{02}$	22,532.20	−0.16	22,399.29	−0.14	22,335.15	−0.18	22,272.81	−0.25	22,152.47	−0.09
$3_{22} \leftarrow 2_{21}$	22,539.47	0.18	22,406.42	0.23	22,342.37	0.36	22,279.81	0.15	22,159.27	0.25
$3_{21} \leftarrow 2_{20}$	22,546.37	0.17	22,413.13	0.18	22,348.99	0.30	22,286.39	0.12	22,165.71	0.23
$3_{12} \leftarrow 2_{11}$	22,926.00	−0.07	22,788.47	0.00			22,657.68	−0.11	22,533.17	0.09
$4_{14} \leftarrow 3_{13}$	29,531.62	−0.16	29,360.21	−0.23	29,277.51	−0.27	29,197.15	−0.23	29,041.86	−0.18
$4_{04} \leftarrow 3_{03}$	30,034.68	−0.40	29,857.62	−0.41	29,722.25	−0.40	29,689.25	−0.45	29,528.90	−0.31
$4_{23} \leftarrow 3_{22}$	30,051.09	0.06	29,873.67	0.07	29,788.15	0.10	29,704.91	−0.02	29,544.27	0.17
$4_{31} \leftarrow 3_{30}$	30,056.46	0.60	29,878.92	0.60	29,793.36	0.64	29,710.09	0.55	29,549.33	0.73
$4_{32} \leftarrow 3_{31}$	30,056.46	0.64	29,878.92	0.64	29,793.36	0.68	29,710.09	0.58	29,549.33	0.76
$4_{22} \leftarrow 3_{21}$	30,068.38	0.04	29,890.55	0.05	29,804.74	−0.01	29,721.44	−0.01	29,560.41	0.16
$4_{13} \leftarrow 3_{12}$	30,565.72	−0.34	30,382.39	−0.25	30,293.98	−0.26	30,208.07	−0.38		
$5_{15} \leftarrow 4_{14}$	36,911.02	−0.51	36,696.83	−0.60	36,493.47	−0.67	36,493.09	−0.59	36,299.03	−0.53
$5_{14} \leftarrow 4_{13}$	38,203.53	−0.75	37,974.47	−0.61	37,863.96	−0.67	37,756.63	−0.79	37,549.27	−0.42
$5_{14} \leftarrow 5_{05}$[c]	30,962.19	0.00	30,956.05	0.00	30,953.4	0.00	30,950.61	0.00	30,945.7	0.00
$6_{15} \leftarrow 6_{06}$	31,784.17	−0.20	31,768.30	0.23	31,761.0	0.40	31,752.89	−0.38		
$7_{16} \leftarrow 7_{07}$	32,762.42	−0.48	32,734.28	0.00			32,707.92	−0.23		
$8_{17} \leftarrow 8_{08}$	33,905.66	−0.76	33,863.11	−0.04	33,842.95	0.07	33,822.96	−0.57	33,785.34	0.10
$9_{18} \leftarrow 9_{09}$	35,223.57	−1.01	35,164.05	−0.04			35,107.94	−0.69	35,054.79	−0.09

[a] Only the A state frequencies are listed. [b] $\Delta\nu = \nu_{obsd} - \nu_{calcd}$ where the calculated frequency was obtained from the rotational constants listed in Table II. [c] Transition used to calculate the rotational constants.
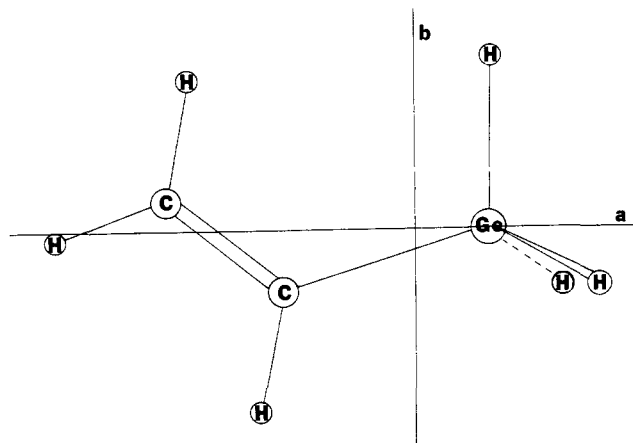

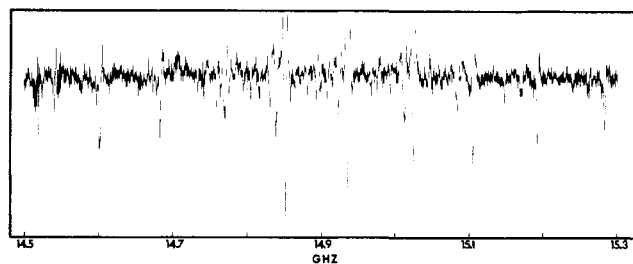Figure 1. A schematic drawing of vinylgermane.

Figure 2. Rotational transitions of the $J = 2 \leftarrow 1$ a-type R branches of five isotopic species of vinylgermane.

provide some information for similar comparisons on these germanium compounds.

Experimental Section

The samples of CH$_2$CHGeH$_3$ and CH$_2$CHGeD$_3$ used in this study were provided by J. B. Turner. The method of preparation was given previously.[14] The microwave spectrum was studied at Dry Ice temperature in the 12.4–40.0-GHz frequency region on a Hewlett-Packard 8460A MRR spectrometer. The Stark cell was modulated with a frequency of 33.3 kHz. In favorable cases, the frequency measurements were accurate to 0.03 MHz.

Microwave Spectra

The spectrum of vinylgermane was initially predicted from the combined structure of vinylsilane[18] and methylgermane[5] with C_s molecular symmetry and the rigid rotor model. The molecule is shown in the principal axis system with the center of mass at the origin (see Figure 1). It is seen that the a and b axes lie in the symmetric plane whereas the c axis is perpendicular to it. Due to the symmetry, only a- and b-type transitions were expected. The observed spectrum is typical of a nearly symmetric prolate top and is in qualitative agreement with the initial predictions. The spectrum resulting from the a-type transitions was

much stronger than that originating from the b-type transitions, and it was easily assigned. There are five naturally abundant isotopic species of germanium with a percentage of 7.7, 36.5, 7.7, 27.4, and 20.5 for the ^{76}Ge, ^{74}Ge, ^{73}Ge, ^{72}Ge, and ^{70}Ge isotopes, which give approximately constant frequency separations and the predicted ratio of intensities. In addition to the Stark patterns, these constant frequency separations and intensity relations between the corresponding transitions of different isotopic species provided excellent data for assigning the spectrum. In Figure 2 is shown the low resolution spectrum of the $J = 2 \leftarrow 1$ a-type transition of CH$_2$CHGeH$_3$. Each ground state line is surrounded by a number of weaker lines which are attributed to vibrational satellites. The splittings of the ground state lines were resolved with the exception of the $K_{-1} = 0$ transitions whose splittings due to the internal rotation of the GeH$_3$ group are too small to be observed with our present experimental equipment. The b-type transitions of the CH$_2$CHGeH$_3$ molecule were observed with larger splittings due to the internal rotation. The spectrum of the $5_{14} \leftarrow 5_{05}$ transition is shown in Figure 3 and the analysis of the internal rotation splitting will be presented in a later section. In Table I are listed the observed ground state rotational transitions for CH$_2$CHGeH$_3$, and in Table II are listed the rotational constants calculated from the ground state transitional frequencies. Also listed in Table II are the moments of inertia and the inertial defect ($\Delta = I_a + I_b - I_c$). Within our experimental accuracy the values of Δ are constant for the different isotopes of germanium. Thus, it is clear that

Table II. Observed Rotational Constants (MHz), Moments of Inertia ($\mu \cdot Å^2$),[a] and κ Values for Ten Isotopic Species of Vinylgermane

	A	B	C	I_a	I_b	I_c	κ	Δ^b
$CH_2CH^{70}GeH_3$	32,731.06	3885.84	3627.26	15.4403	130.056	139.328	−0.982230	6.168
$CH_2CH^{72}GeH_3$	32,726.53	3862.15	3606.59	15.4424	130.854	140.126	−0.982448	6.170
$CH_2CH^{73}GeH_3$	32,724.49	3850.73	3596.61	15.4434	131.242	140.515	−0.982551	6.170
$CH_2CH^{74}GeH_3$	32,721.94	3839.67	3586.89	15.4446	131.620	140.896	−0.982648	6.169
$CH_2CH^{76}GeH_3$	32,718.37	3818.19	3568.14	15.4463	132.360	141.636	−0.982844	6.170
$CH_2CH^{70}GeD_3$		3684.29	3456.31		137.171	146.219		
$CH_2CH^{72}GeD_3$		3665.14	3439.42		137.888	146.937		
$CH_2CH^{73}GeD_3$		3655.90	3431.24		138.236	147.287		
$CH_2CH^{74}GeD_3$		3646.90	3423.29		138.577	147.629		
$CH_2CH^{76}GeD_3$		3629.45	3407.88		139.243	148.297		

[a] Conversion factor: 505,377 MHz·μ·$Å^2$. [b] $\Delta = I_a + I_b - I_c$.

Table III. Observed Ground-State Transition Frequencies (MHz) for Vinylgermane-d_3

Transition	—$CH_2CH^{70}GeD_3$—		—$CH_2CH^{72}GeD_3$—		—$CH_2CH^{73}GeD_3$—		—$CH_2CH^{74}GeD_3$—		—$CH_2CH^{76}GeD_3$—	
	ν (obsd)^a	$\Delta\nu^b$	ν (obsd)^a	$\Delta\nu^b$	ν (obsd)^a	$\Delta\nu^b$	ν (obsd)^a	$\Delta\nu^b$	ν (obsd)^a	$\Delta\nu^b$
$2_{12} \leftarrow 1_{11}$	14,053.23^c	0.00	13,983.40^c	0.00	13,949.80^c	0.19	13,916.78^c	0.00	13,853.20^c	0.10
$2_{02} \leftarrow 1_{01}$	14,279.25^c	0.00	14,207.23^c	0.00	14,172.40^c	−0.01	14,138.52^c	0.00	14,072.84^c	−0.02
$2_{11} \leftarrow 1_{10}$	14,509.18^c	0.00	14,434.84^c	0.00	14,399.12^c	0.18	14,363.99^c	0.00	14,296.33^c	0.10
$3_{13} \leftarrow 2_{12}$	21,078.52	−0.10	20,973.81	−0.11	20,923.19^c	−0.06	20,873.94	−0.07	20,778.56^c	0.04
$3_{03} \leftarrow 2_{02}$	21,413.88	−0.10	21,305.93	−0.11	21,253.79^c	−0.02	21,202.98	−0.14	21,104.65^c	−0.10
$3_{22} \leftarrow 2_{21}$	21,421.67	−0.13	21,313.59	−0.18	21,261.33^c	−0.08	21,210.50	−0.08		
$3_{21} \leftarrow 2_{20}$	21,429.50	−0.12	21,321.19	−0.09	21,268.82	−0.04	21,217.94	−0.10	21,119.16^c	−0.10
$3_{12} \leftarrow 2_{11}$	21,762.44	−0.10	21,650.98	−0.05	21,597.18^c	−0.05	21,544.70	−0.11	21,443.25^c	0.04
$4_{14} \leftarrow 3_{13}$	28,102.31	−0.27	27,962.76	−0.29	27,895.26	−0.26	27,829.62	−0.24	27,702.78	0.17
$4_{04} \leftarrow 3_{03}$	28,542.66	−0.21	28,398.91	−0.43	28,329.42	−0.50	28,261.80	−0.33	28,131.00	−0.21
$4_{23} \leftarrow 3_{22}$	28,560.60	−0.28	28,416.47	−0.30	28,346.85	−0.24	28,279.04	−0.28	28,147.81	−0.12
$4_{31} \leftarrow 3_{30}$	28,565.94	−0.41	28,421.72	−0.33	28,351.99	−0.31	28,284.17	−0.36	28,153.19^c	0.20
$4_{32} \leftarrow 3_{31}$	28,565.94	−0.35	28,421.72	−0.27	28,351.99	−0.25	28,284.17	−0.30	28,153.19^c	0.26
$4_{22} \leftarrow 3_{21}$	28,579.97	−0.64	28,435.46	−0.20	28,365.57	−0.14	28,297.64	−0.32		
$4_{13} \leftarrow 3_{12}$	29,014.08	−0.34	28,865.57	−0.30	28,793.90	−0.22	28,723.88	−0.34	28,588.65^c	−0.16
$5_{15} \leftarrow 4_{14}$	35,124.02	−0.84	34,949.64	−0.69	34,865.50	−0.47			34,624.44	−0.48
$5_{05} \leftarrow 4_{04}$	35,663.44	−0.51	35,484.05	−0.99	35,397.33	−1.13	35,312.95	−0.75	35,149.58	−0.87
$5_{24} \leftarrow 4_{23}$	35,698.00	−0.67	35,517.90	−0.70	35,430.82	−0.72	35,346.13	−0.68	35,182.14	−0.50
$5_{42} \leftarrow 4_{41}$	35,706.51	−0.85	35,526.20	−0.80	35,439.11	−0.71	35,354.33	−0.78	35,190.18	−0.52
$5_{41} \leftarrow 4_{40}$	35,706.51	−0.86	36,526.20	−0.80	35,439.11	−0.71	35,354.33	−0.78	35,190.18	−0.52
$5_{23} \leftarrow 4_{32}$	35,708.95	−0.67	35,528.65	−0.54	35,441.47	−0.31	35,356.68	−0.59	35,192.50	−0.30
$5_{32} \leftarrow 4_{31}$	35,708.95	−0.89	35,528.65	−0.75	35,441.47	−0.71	35,356.68	−0.80	35,192.50	−0.49
$5_{23} \leftarrow 4_{22}$	35,736.91	−0.81	35,556.03	−0.33	35,468.97	−0.22	35,383.52	−0.56		
$5_{14} \leftarrow 4_{13}$	36,263.64	−0.65	36,078.03	−0.70	35,988.29	−0.80	35,900.99	−0.72	35,731.99^c	−0.56

[a] No splittings were observed for the listed transitions. [b] $\Delta\nu = \nu_{obsd} - \nu_{calcd}$. [c] Frequency used to calculate the rotational constants.
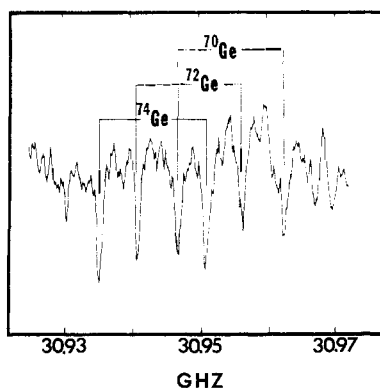

Figure 3. Rotational transitions of the $J = 5_{14} \leftarrow 5_{05}$ b-type Q branches of five isotopic species of vinylgermane.

the germanium atom is located on the symmetry plane.

In contrast to the microwave spectrum of CH_2CHGeH_3, some extra bands were observed in the spectrum of CH_2CHGeD_3 which can be attributed to an impurity. The presence of the impurity in CH_2CHGeD_3 is believed to be the reason for the weaker spectrum of this compound when observed at the identical experimental conditions as used in recording the spectrum of CH_2CHGeH_3. In Table III, are listed the observed rotational transitions for vinylgermane-d_3. The spectrum obtained is very similar to that for vinyl-

germane but no internal rotational splitting was observed because of the larger value of I_α for the GeD_3 top. Since all the measured a-type transitions are rather insensitive to the rotational constant A and no assignment of the b-type transition was made on this species, only the rotational constants B and C are listed in Table II (the sample was lost in an explosion).

All assignments were substantiated by a rigid rotor fit of the frequencies for the ground state transitions. The differences in the observed and calculated values for the ground state transitions are listed in Tables I and III for CH_2CHGeH_3 and CH_2CHGeD_3, respectively. The accuracy of the rotational constant A is 0.5 MHz while that of the rotational constants B and C is 0.03 MHz.

Structure

The present experimental information on the rotational constants of only ten isotopic species does not allow a complete determination of the r_s structure or the conformation of the germyl group in vinylgermane. As shown in Table II, the inertial defect of CH_2CHGeH_3 agrees with the value expected for a planar heavy atom skeleton and the out-of-plane hydrogens of the germyl moiety. The constancy of the inertial defect for different isotopic species of germanium also favors a planar heavy atom structure. It seems reasonable to assume that the germyl group is staggered to the CH bond of the central carbon which is similar to the conformation found for propylene[16] and vinylsilane.[18] In an at-

Table IV. Structure of Vinylgermane

⌐————Assumed————¬		⌐————Calculated————¬	
C–H (cis)	1.097 Å	C=C	1.347 ± 0.015 Å
C–H (trans)	1.097 Å	Ge—C	1.926 ± 0.012 Å
C–H	1.094 Å	Ge—H	1.520 ± 0.005 Å
∠CCH (cis)	120.35°	∠CCGe	122.9 ± 0.6°
∠CCH (trans)	120.65°	∠CGeH	109.7 ± 0.6°
∠CCH	118.00°		

Table V. Stark Coefficients ((MHz cm²)/V²) and Dipole Moments of $CH_2CH^{74}GeH_3$

Transitions	$|M|$	⌐——$\Delta\nu/E^2$ (× 10⁵)——¬	
		Obsd	Calcd
$3_{13} \leftarrow 2_{12}$	1	0.66	0.68
	2	3.15	3.12
$3_{12} \leftarrow 2_{11}$	1	−0.76	−0.75
	2	−2.93	−2.95

$|\mu_a| = 0.49 \pm 0.02$ D $\qquad |\mu_c| = 0$ (by symmetry)
$|\mu_b| = 0.12 \pm 0.02$ D $\qquad |\mu_t| = 0.50 \pm 0.03$ D

Table VI. Internal Rotation Splittings $\Delta\nu = \nu_E - \nu_A$ (MHz) Calculated from $v = 0$ Transitions

Transition	⌐——$CH_2CH^{74}GeH_3$——¬			⌐——$CH_2CH^{72}GeH_3$——¬			⌐——$CH_2CH^{70}GeH_3$——¬		
	$\Delta\nu$ (obsd)	$\Delta\nu$ (calcd)ᵃ	V_3 (cm⁻¹)	$\Delta\nu$ (obsd)	$\Delta\nu$ (calcd)ᵃ	V_3 (cm⁻¹)	$\Delta\nu$ (obsd)	$\Delta\nu$ (calcd)ᵃ	V_3 (cm⁻¹)
$2_{12} \leftarrow 1_{11}$	1.13	1.14	433.1	1.10	1.12	433.5	1.14	1.15	432.9
$2_{11} \leftarrow 1_{10}$	−1.15	−1.19	434.7	−1.17	−1.17	433.3	−1.17	−1.20	433.3
$3_{13} \leftarrow 2_{12}$	0.29	0.29	433.6	0.27	0.28	434.2	0.26	0.29	432.6
$3_{12} \leftarrow 2_{11}$	−0.37	−0.36	432.2	−0.36	−0.35	432.9	−0.36	−0.36	432.9
$4_{13} \leftarrow 3_{12}$	−0.19	−0.21	436.9	−0.18	−0.21	437.4	−0.19	−0.21	435.9
$5_{14} \leftarrow 4_{13}$	−0.18	−0.18	432.5	−0.18	−0.18	432.5	−0.18	−0.18	432.5
$5_{14} \leftarrow 5_{05}$	−15.46	−14.7	430.0	−15.49	−14.59	429.9	−15.86	−14.7	428.5
	$\bar{V}_3 = 432.9 \pm 1.8$ cm⁻¹			$\bar{V}_3 = 433.4 \pm 2.2$ cm⁻¹			$\bar{V}_3 = 432.7 \pm 2.2$ cm⁻¹		

ᵃ Calculated from $F = 4.320$ cm⁻¹, $\alpha = 0.3829$, $\beta = 0.0140$, and the corresponding $\bar{V}_3$.

tempt to obtain the molecular structure from the experimental rotational constants, a computer program was written in this laboratory to do a least-squares fit of the structural parameters to the observed rotational constants. As shown in Figure 1, it was assumed that the C–H (cis), C–H (trans), and C–H bond distances and the CCH (cis), CCH (trans), and CCH angles were identical with those of vinylsilane, and the C÷Ge bond was along the symmetry axis of the germyl moiety. A best fit to the rotational constants was obtained by adjusting the remaining structural parameters. In these calculations, it was found that the C—Ge—H angle and the Ge—H bond distance were dependent appreciably on the rotational constant A whereas the C=C—Ge angle and the C—Ge distance were more dependent on the B and C rotational constants.

The resultant structure yielded values for all of the rotational constants within 0.5 MHz of the observed values. The structural parameters for vinylgermane are tabulated in Table IV. The uncertainties are estimated mainly from different assumptions in the C—H distances and the H—C—C angles. The C=C bond distance is essentially in agreement with those of propylene[16] and vinylsilane.[18] The Ge—C bond distance is shorter than the Ge—C bond of methylgermane[5] and will be discussed later.

Dipole Moment

The ground state transitions of CH_2CHGeH_3 were observed to have quadratic Stark effects. Measurements were made for the $|M| = 1$ and 2 components of the $3_{13} \leftarrow 2_{12}$ transition and the $|M| = 1$ and 2 components of the $3_{12} \leftarrow 2_{11}$ transition. Field calibration was done by measuring the $M = 0$ component of OCS for the $J = 2 \leftarrow 1$ transition.[21] The observed and the calculated Stark coefficients are listed in Table V for the molecule $CH_2CH^{74}GeH_3$. From these measurements, the following values were determined: $|\mu_a| = 0.49 \pm 0.02$, $|\mu_b| = 0.12 \pm 0.02$, and $|\mu_{total}| = 0.50 \pm 0.03$ D. The measured values of the dipole moment components explain why it was easier to observe a-type than b-type transitions.

The resultant dipole moment makes an angle of $14 \pm 3°$ with the a axis. From the structure the a-axis makes an angle of 17° to the C-Ge bond. Thus, the angle between the resultant dipole and the C-Ge bond is either $31 \pm 3°$ or $3 \pm$

3°. Since the Ge atom is very close to the a-axis, the germanium isotopic substitution does not make any significant change in the orientation of the a-axis, and thus it was impossible to determine which angle is correct from our present information.

Internal Rotation

Some of the rotational transitions for vinylgermane (CH_2CHGeH_3) were split into A and E states due to the internal rotation of the germyl group. An analysis of the internal rotational splitting was made with the aid of a computer program written by Laurie and Lau. The program adopts the "principal axis method," and the products of the Mathieu eigenfunctions and the symmetric top wave functions are used as basis functions for the matrix representations. The internal rotational parameters $F = 4.320$ cm⁻¹, $\alpha = 0.3829$, and $\beta = 0.0140$ were calculated from the molecular structure listed in Table IV. It is assumed that these parameters are essentially the same for the different isotopic species of germanium because of the nearness of the Ge atom to the principal a-axis and the small angle between the Ge-C bond and the a-axis. Analysis of the internal rotation can, therefore, be made by taking constant values of F, α, and β for the different isotopic species of Ge. In Table VI are summarized the internal rotation calculations. The values under column V_3 are calculated from the splitting of the corresponding individual rotational transition. The average values of $\bar{V}_3$ for $CH_2CH^{74}GeH_3$, $CH_3CH^{72}GeH_3$, and $CH_3CH^{70}GeH_3$ are the same within the standard deviation. It is believed that the deviations come from the uncertainty in the molecular structure. This uncertainty is estimated to be ±20 cm⁻¹.

Internal rotational splittings for $CH_2CH^{73}GeH_3$ and $CH_2CH^{76}GeH_3$ in the $v = 0$ state were also observed. No analysis of internal rotation was undertaken for these two species because the observed splittings were very close to the splittings for the other species and it was believed that the barrier height would be the same.

First excited torsional state transitions of CH_2CHGeH_3 were observed with much larger splittings than the ground state transitions. Frequency measurements for these excited states were carried out for $CH_2CH^{74}GeH_3$ only. In Table

Table VII. Internal Rotational Splittings from $v = 1$ Torsional State Transitions of $CH_3CHGeH_3{}^a$

Transition	ν_A (obsd)	$\Delta\nu^b$ (obsd)	$\Delta\nu^b$ (calcd)	V (cm^{-1})
$3_{13} \leftarrow 2_{12}$	21,892.97	171.91	173	434.4
$3_{12} \leftarrow 2_{11}$	22,625.44	-168.39	-170	435.1
$4_{14} \leftarrow 3_{13}$	29,188.59	124.87	125	433.8
$4_{13} \leftarrow 3_{12}$	30,165.19	-119.16	-120	433.9
$5_{15} \leftarrow 4_{14}$	36,482.60	80.67	80	433.3
$5_{14} \leftarrow 4_{13}$	33,703.12	-74.51	-70	431.8
			$\bar{V} = 433.7 \pm 1.1$ cm^{-1}	

^{a} All frequencies are in units of MHz. ^{b} $\Delta\nu = \nu_E - \nu_A$.

VII are given the observed transitional frequencies of the $v = 1$ torsional state with the accompanying splittings. Calculations were made by the identical method as stated earlier for the ground state internal rotational splittings. The same molecular structure was assumed in the first torsional excited state as in the ground state. As shown in the table, the barrier height obtained ($\bar{V}_3 = 433.7$ cm^{-1}) is in excellent agreement with the value of the barrier ($\bar{V}_3 = 432.9$ cm^{-1}) obtained from the ground state splittings.

Discussion

Similar to the results obtained by O'Reilly and Pierce[18] for the vinylsilane molecule, the Ge–C bond distance (1.926Å) in vinylgermane is smaller than the corresponding Ge–C bond distance (1.9453Å) of methylgermane.[5] This difference (0.02Å) is probably meaningful even though the methods for obtaining the structural parameters are different. Assuming hyperconjugation has no effect on the Ge–C distance, the Ge–C bond distance in vinylgermane can be interpreted as the sum of the covalent radii of sp^3 germane and sp^2 carbon whereas the corresponding bond distance in methylgermane can be interpreted as the sum of the covalent radii of sp^3 germane and sp^3 carbon. The difference in the Ge–C bond distances between these two molecules can thus be explained on the basis of the difference in the covalent radii of sp^2 and sp^3 carbons. The value (0.02Å) is in good agreement with that calculated by Mulliken.[22] It is interesting to note, that within experimental error, the difference in the Ge–C bonds is comparable to the difference in the Si–C bonds between vinylsilane (1.853Å)[18] and methylsilane (1.488Å).[20]

The spectrum of $CH_2CH^{73}GeH_3$ was observed and measured, and, since the nuclear spin of the ^{73}Ge nucleus is $\%_2$, splitting of the rotational transitions due to quadrupole coupling is expected. Experimentally, no resolvable quadrupole components were observed and no accurate quadrupole coupling constants could be determined. By measuring the line widths of several transitions not split by internal rotation, the quadrupole coupling constant $|\chi_{aa}|$ is estimated to be less than 2.8 MHz. The small interaction between the nuclear spin and the molecular rotation implies that the electronic density around the Ge atom is nearly spherically distributed. Thus, it favors our preceding discussion on the Ge–C bond distance being based on the sp^3 hybridization of Ge.

The shortening of the Ge–C bond distance in vinylgermane may also be accounted for by hyperconjugation. The hyperconjugated structure such as $H_3{}^+Ge=^-CH=CH_2$ indicates that the germyl group acts as a donor and the Ge–C bond as an acceptor. The donor bond length is expected to be slightly increased and the acceptor bond length to be decreased. In the present work, the expected increase in the Ge–H bond distance is probably so small that it would be absorbed in the experimental uncertainty.

The internal rotational barrier of 1238 ± 57 cal/mol in vinylgermane is the same as that found for methylgermane.[5] It is expected that as the distance increases between the vinyl and rotor groups, the decrease in the number of $H \cdots H$ interactions will become less significant. Also, the C–Ge internal rotational barriers are not expected to be significantly affected by the substituents as compared to the corresponding silicon and carbon compounds. Therefore, the fact that the internal rotational barriers are the same in methylgermane and vinylgermane is consistent with the "long" C–Ge distance compared to the C–Si or C–C distances.

References and Notes

(1) For part XVI, see J. R. Durig, Y. S. Li, and J. B. Turner, *Inorg. Chem.*, **13**, 1495 (1974).
(2) Author to whom correspondence should be addressed.
(3) Taken in part from the thesis of K. L. Kizer, submitted to the Department of Chemistry in partial fulfillment of the Ph.D., Aug 1971.
(4) A. I. Baruchov and A. M. Prokhorov, *Opt. Spektrosk.*, **4**, 799; **5**, 530 (1958).
(5) V. W. Laurie, *J. Chem. Phys.*, **30**, 1210 (1959).
(6) A. I. Baruchov and Y. N. Petrov, *Opt. Spektrosk.*, **11**, 129 (1961).
(7) E. C. Thomas and V. W. Laurie, *J. Chem. Phys.*, **50**, 3512 (1969).
(8) N. A. Irisova and E. M. Dianov, *Opt. Spektrosk.*, **9**, 261 (1960).
(9) J. R. Durig, M. M. Chen, Y. S. Li, and J. B. Turner, *J. Phys. Chem.*, **77**, 227 (1973).
(10) Y. S. Li and J. R. Durig, *Inorg. Chem.*, **12**, 306 (1973).
(11) E. C. Thomas and V. W. Laurie, *J. Chem. Phys.*, **51**, 4327 (1969).
(12) J. R. Durig and K. L. Hellams, *J. Mol. Spectrosc.*, submitted 1974.
(13) E. O. Schlemper and D. Britton, *Inorg. Chem.*, **5**, 511 (1966).
(14) J. R. Durig and J. B. Turner, *Spectrochim. Acta, Part A*, **27**, 1623 (1971).
(15) D. R. Lide and D. E. Mann, *J. Chem. Phys.*, **27**, 868 (1957).
(16) D. R. Lide and D. Christensen, *J. Chem. Phys.*, **35**, 1374 (1961).
(17) A. E. Hirota, *J. Chem. Phys.*, **45**, 1984 (1966).
(18) J. M. O'Reilly and L. Pierce, *J. Chem. Phys.*, **34**, 1176 (1961).
(19) S. Weiss and·G. E. Leroi, *J. Chem. Phys.*, **48**, 962 (1968).
(20) R. W. Kilb and L. Pierce, *J. Chem. Phys.*, **27**, 108 (1957).
(21) J. S. Muenter, *J. Chem. Phys.*, **48**, 4544 (1968).
(22) R. S. Mulliken, *Tetrahedron*, **6**, 68 (1959).